analytical chemistry

pubs.acs.org/ac Article

Multiplex Asymmetric PCR by Combining the Amplification Refractory Mutation System with the Homo-Tag-Assisted Nondimer System

Ying Liu,[#] Yinghua Liu,[#] Liu Guo, Yazhe Wu, Yafang Wang, Lingzhen Xu, Mingzhu Xu, Siyu Huang, Ping Chen, Ting Wang, Qiuying Huang,* and Qingge Li*

Cite This: *Anal. Chem.* 2024, 96, 9200−9208 Read Online

ACCESS | Metrics & More | Article Recommendations | Supporting Information

ABSTRACT: Asymmetric PCR is widely used to produce single-stranded amplicons (ss-amplicons) for various downstream applications. However, conventional asymmetric PCR schemes are susceptible to events that affect primer availability, which can be exacerbated by multiplex amplification. In this study, a new multiplex asymmetric PCR approach that combines the amplification refractory mutation system (ARMS) with the homo-Tag-assisted nondimer system (HANDS) is described. ARMS-HANDS (A-H) PCR utilizes equimolar-tailed forward and reverse primers and an excess Tag primer. The tailed primer pairs initiate exponential symmetric amplification, whereas the Tag primer drives linear asymmetric amplification along fully matched strands but not one-nucleotide mismatched strands, thereby generating excess ss-amplicons. The production of ss-amplicons is validated using agarose gel electrophoresis, sequencing, and melting curve analysis. Primer dimer alleviation is confirmed by both the reduced Loss function value and a 20-fold higher sensitivity in an 11-plex A-H PCR assay than in an 11-plex conventional asymmetric PCR assay. Moreover, A-H PCR demonstrates unbiased amplification by its allele quantitative ability in correct identification of all 31 trisomy 21 samples among 342 clinical samples. A-H PCR is a new generation of multiplex asymmetric amplification approach with various applications, especially when sensitive and quantitative detection is required.

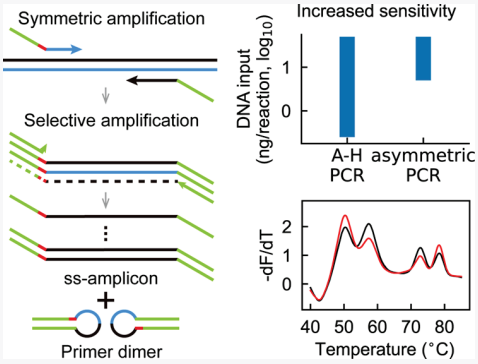

Nucleic acid detection often relies on the hybridization between a target and a probe DNA molecule both in a single-stranded form. The single-stranded target DNA molecules can be generated through various approaches, among which asymmetric PCR is theoretically the simplest, owing to the omission of physical, chemical, or enzymatic denaturation. Asymmetric PCR preferentially amplifies one strand of the original DNA more than the other, leading to the generation of single-stranded amplicons (ss-amplicons).[1] During the early stages, amplification occurs exponentially as symmetric PCR, yielding double-stranded amplicons (ds-amplicons). Once the limiting primer is depleted in the reaction, exponential amplification switches to linear amplification with the available excess primer, forming ss-amplicons. Asymmetric PCR can be used for probe-based melting curve analysis,[2−4] direct Sanger sequencing,[1] paper-based nucleic acid diagnostics,[5] molecular-beacon-based-post-PCR visualization detection,[6] and for improving the detection signals of microarray[7] and molecular beacon-based real-time PCR detection.[8]

However, asymmetric PCR generates fewer amplicons than conventional symmetric PCR; thus, it has an overall lower analytical sensitivity. Additionally, when the reaction is controlled by a limiting primer, any events affecting primer availability, such as primer dimer (PD) formation or low levels of nonspecific binding, can cause substantial variations in the primer content during the linear phase, posing challenges to the reproducibility of the amplification process. These effects are exacerbated when multiple primer pairs undergo multiplex amplification in one reaction vessel, where the appropriate conditions are more difficult to optimize, leading to unbalanced amplification and low target detection sensitivity. Recognition of the reduced melting temperature (T_m) of the limiting primer led to the development of linear after-the-exponential (LATE)-PCR, which renders asymmetric PCR assays as efficient as symmetric PCR assays, regardless of the primer ratio.[9] Further improvements toward flexible designs have facilitated the establishment of different two-stage asymmetric PCR approaches,[10−12] all of which have achieved increased analytical sensitivity compared with conventional

Received: March 11, 2024
Revised: May 7, 2024
Accepted: May 9, 2024
Published: May 21, 2024

Downloaded via COPYRIGHT CLEARANCE CTR DCMT DLVRY on August 8, 2025 at 15:49:23 (UTC).
See https://pubs.acs.org/sharingguidelines for options on how to legitimately share published articles.

ACS Publications © 2024 American Chemical Society

https://doi.org/10.1021/acs.analchem.4c01322
Anal. Chem. 2024, 96, 9200−9208

Tecan Ex. 2142, Page 1 of 9
QIAGEN Sciences, LLC v. Tecan Genomics - IPR2025-00028

asymmetric PCR. However, the application of these improved approaches in multiplex assays remains unclear.

Multiplex PCRs face challenges such as PD formation and unequal amplification rates, which are influenced by amplicon length, sequence, and priming efficiency. The PD effect intensifies during the simultaneous amplification of many loci because the number of potential primer−primer interactions increases roughly with the square of the number of loci.[13] Several approaches have been introduced to improve PCR multiplexing beyond the traditional limit of several dozen loci per reaction.[14,15] Among them, the homo-Tag-assisted non-dimer system (HANDS) utilizes several cycles of genomic priming followed by cycles of universal priming. The switch from genomic to universal priming was accomplished by increasing the annealing temperature and designing a genome-specific portion of the primers with a lower T_m than that of the universal Tag primers. Variations of this universal primer-based multiplex PCR have been successfully used for large-scale array-based single nucleotide polymorphism (SNP) discovery and genotyping assays.[16] However, HANDS is a stringent symmetric PCR because the single Tag primer functions equally on both ends of the amplicons. To take advantage of the PD alleviation of HANDS, half of the primers (either forward or reverse) were reportedly concatenated to a 5′-universal Tag sequence (also known as a 'tail' sequence) for multiplex asymmetric PCR in microarray detections.[5,17] Because the other half of the primers were unprotected from PD formation, extensive optimization was still needed to increase analytical sensitivity, highlighting the need to further advance multiplex asymmetric PCR by removing PD from the reaction.

We aimed to develop a generic multiplex asymmetric PCR approach with a simple design, easy optimization, high sensitivity, and balanced amplification. Our strategy involves integrating the amplification refractory mutation system (ARMS) into HANDS, ensuring that all reverse primers carry a tail that is identical to Tag sequence, while all forward primers carry a tail with a one-nucleotide difference at the 3′-end. Exponential symmetric amplification occurred because of the equimolar-tailed forward and reverse primers. In contrast, linear asymmetric amplification was driven by the single Tag primer along the matched strands but not one-nucleotide mismatched strands based on ARMS, thereby generating ss-amplicons oriented in the same direction as the reverse primers. Meanwhile, the accumulation of PDs was alleviated owing to the formation of the panhandle structure based on HANDS. Combining both ARMS and HANDS in one reaction, we term this new scheme ARMS-HANDS (A-H) PCR. Our study demonstrated that this simple scheme not only provides high analytical sensitivity in multiplex detection but also enables accurate allele quantification of multiple SNPs.

MATERIALS AND METHODS

Oligonucleotides. All synthetic oligonucleotides (Sangon Biotech, Shanghai, China) are listed in Tables S1−S6.

Human Genomic DNA (gDNA) Samples and Clinical Samples. A collection of 87 normal human gDNA samples stored in our laboratory was used as a diploidy control. gDNA was extracted using either the phenol−chloroform method or the paramagnetic particle method [Lab-Aid 824 Nucleic Acid Extraction System (Zeesan Biotech, Xiamen, China)]. Two purified trisomy 21 human gDNA samples (NA01921 and NA01137; Coriell Institute for Medical Research, Camden, NJ, USA) were used as trisomy controls. A total of 234 amniotic fluid and 108 chorionic villus samples were collected at Suzhou Municipal Hospital during routine prenatal diagnosis using chromosomal microarray analysis (CMA) and karyotyping. gDNA from these clinical samples was extracted using a QIAamp DNA Mini Kit (QIAGEN, Hilden, Germany). The concentrations of all samples were adjusted (10 ng/μL unless otherwise indicated) using an ND-2000 spectrophotometer (NanoDrop Technologies Inc., Wilmington, DE) before use. The collection of specimens and associated clinical data used in this study were approved by the Research Ethics Committee of Xiamen University (XDYX2021026). All of the experiments were performed in accordance with the Declaration of Helsinki, and informed consent was obtained from the individual patients or their guardians.

Singleplex PCR. Each singleplex PCR was performed in a 25-μL solution containing 1 × PCR master buffer, 3 mM $MgCl_2$, 0.16 mM dNTP mixture, 1.0 U *Taq* HS DNA polymerase (TaKaRa, Dalian, China), 0.25 U uracil-*N*-glycosylase (Thermo Fisher Scientific, Wilmington, DE), 5 μL (∼1 ng/μL) human gDNA or water, 0.2 μM the molecular beacon probe, 0.06 μM tailed primers and 0.6 μM the Tag primer for HANDS and A-H PCR, or 0.06 μM the limiting primer and 0.6 μM the excess primer for asymmetric PCR (sequences and concentrations are listed in Tables S1 and S2). PCR and melting curve analysis were performed using an SLAN 96S real-time PCR instrument (Hongshi Medical Technology Co. Ltd., Shanghai, China) as follows: 50 °C for 2 min; 95 °C for 5 min; 6 cycles of 95 °C for 15 s, 53 °C for 15 s, and 76 °C for 20 s; 50 cycles of 95 °C for 15 s, 58 °C for 15 s, and 76 °C for 20 s; followed by 95 °C for 1 min, 37 °C for 3 min, and finally, a temperature increase from 40 to 85 °C (0.04 °C/step). Fluorescence from the Cy5 channel was recorded during the annealing step of the second set of 50 amplification cycles and at each step of the continuous temperature increase during melting curve analysis.

PCR products were analyzed by 4% agarose gel electrophoresis. Subsequently, PCR products were recovered from the agarose gel and subjected to Sanger sequencing (Sangon Inc., Shanghai, China).

Multiplex PCR. Both 11-plex A-H PCR and 11-plex asymmetric PCR for the genotyping of 11 SNPs on human chromosome 21 were performed using a 25-μL solution containing 1 × PCR master buffer, 5.0 mM $MgCl_2$, 0.2 mM dNTP mixture, 2.0 U *Taq* HS DNA polymerase, 0.25 U uracil-*N*-glycosylase, 5 μL of human gDNA or water, 0.2 μM of each probe, 0.03−0.08 μM tailed primers and 2 μM Tag primer for 11-plex A-H PCR, or 0.016−0.11 μM forward primer and 0.4−1.2 μM reverse primer for asymmetric PCR (sequences and concentrations are listed in Table S4). PCR and melting curve analysis were performed using an SLAN 96S real-time PCR instrument (Hongshi Medical Technology Co. Ltd.) as follows: 50 °C for 2 min; 95 °C for 5 min; 6 cycles of 95 °C for 15 s, 53 °C for 15 s, and 76 °C for 20 s; 55 cycles of 95 °C for 15 s, 58 °C (11-plex A-H PCR) or 55 °C (11-plex asymmetric PCR) for 15 s, and 76 °C for 20 s; followed by 95 °C for 1 min, 37 °C for 3 min, and finally, a temperature increase from 40 to 85 °C (0.04 °C/step). Fluorescence from six detection channels (Atto 425, FAM, HEX, ROX, Cy5, Quasar 705) was recorded during the annealing step of the second set of 55 amplification cycles and at each step of the continuous temperature increase during melting curve analysis.

https://doi.org/10.1021/acs.analchem.4c01322
Anal. Chem. 2024, 96, 9200−9208

Tecan Ex. 2142, Page 2 of 9
QIAGEN Sciences, LLC v. Tecan Genomics - IPR2025-00028

The 12-plex, 36-plex, 60-plex, 84-plex, and 108-plex A-H PCR were performed using a 25 μL solution containing 1 × PCR master buffer, 9.0 mM $MgCl_2$, 0.8 mM dNTP mixture, 2.5 U *Taq* HS DNA polymerase, 0.25 U uracil-N-glycosylase, 5 μL of human gDNA or water, 30 nM tailed-specific primers (the 12-plex, 36-plex, 60-plex, 84-plex, and 108-plex A-H PCRs contained primers of loci 1−12, 1−36, 1−60, 1−84, and 1−108, respectively), 5.4 μM Tag primer, and 0.2 μM probes of loci 1−12 (sequences and concentrations are listed in Table S5). One gDNA sample was diluted with water to yield concentrations of 10, 1, 0.5, 0.1, 0.05, and 0.01 ng/μL and analyzed in four replicates. The procedure for PCR and melting curve analysis was identical to that of the 11-plex A-H PCR excepting the second set of 55 cycles was changed to 80 cycles.

Allele Quantification Using the A-H PCR Assay. The allele quantitative ability of the 11-plex A-H PCR was tested by 87 normal gDNA samples, 2 trisomy 21 gDNA samples, a series of gDNA mixtures containing different percentages of trisomy 21 gDNA (0, 10, 20, 30, 40, 50, 60, 70, 80, 90, and 100%), and a series of normal and trisomy 21 gDNA samples with concentrations of 50, 25, 10, and 5 ng/μL. The results were analyzed using MeltPro Manager version 8.2.2 (Hongshi Medical Technology Co. Ltd.) for automatic export of the height of the melting peak (R_m). For heterozygous SNP, the ratio of the melting peak height (HR) was calculated by R_m of the matched allele (R_m2) to R_m of the mismatched allele (R_m1). The HR was normalized by the average HR value of normal gDNA samples, yielding a normalized height ratio (nHR).

Clinical Detection of Trisomy 21. To detect trisomy 21 using the 16 SNPs, 11-plex A-H PCR and an additional 5-plex A-H PCR targeting five SNPs were performed (Table S6). The 5-plex PCR was performed in a 25 μL solution containing 1 × PCR master buffer, 3.0 mM $MgCl_2$, 0.2 mM dNTP mixture, 1.0 U Taq *HS* DNA polymerase, 0.25 U uracil-*N*-glycosylase, and 5 μL of human gDNA. PCR and melting curve analysis was identical to that of the 11-plex A-H PCR. The results were analyzed using MeltPro Manager version 8.2.2, as described for the 11-plex A-H PCR.

Statistical Analysis. Statistical analysis was performed using SPSS version 20.0 (SPSS Inc., Chicago, IL, USA), and a p value <0.05 was considered statistically significant.

RESULTS

The Working Principle of A-H PCR. A-H PCR contains three types of primers: tailed forward primers, tailed reverse primers, and a universal Tag primer. The Tag primer has an identical sequence with the tail sequence of the reverse primers (Tail) and a one-nucleotide difference with the tail sequence of the forward primers (Tail′) at the 3′-end (Figure 1). The concentrations of the tailed primers are at least 10 times lower than that of the Tag primer. As shown in Figure 1A, low concentrations of tailed primers initiate the amplification. After two cycles of genomic priming, reverse complementary tail sequences are incorporated into the amplicons. Subsequent annealing of the Tag primer facilitates its extension along the newly synthesized matched strand but not the one-nucleotide mismatched strand, according to the ARMS mechanism. Such an unbalanced extension generates excess ss-amplicons with the 5′-Tail and 3′-Tail′ complements. Similar to HANDS, the PDs are mainly derived from the nonspecific interactions between tailed primers and Tag primer (shown as species 1 and species 2, Figure 1B) in A-H PCR. As Tail and Tail′ differ by only one nucleotide at the 3′-end, they can be regarded as equivalent in the HANDS mechanism. Once formed, all PDs possess the Tail (or Tail′) sequence on their 5′-ends and the complement of the Tail (or Tail′) sequence on their 3′-ends. As a consequence of the relatively small size of PDs, self-annealing of the complementary ends of single-stranded PDs is preferred because of their high local concentration, which promotes the formation of panhandle structures that restrict the access of the Tag primer for further amplification. Therefore, all the formed PDs cannot be amplified as efficiently as those specific and large sized amplicons.

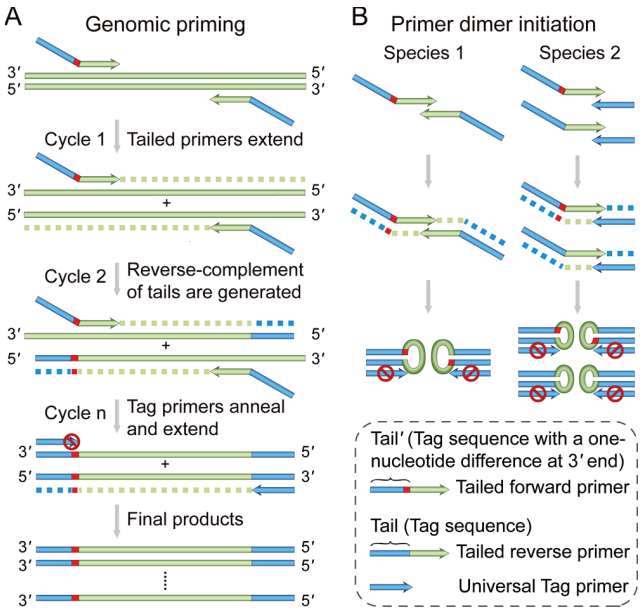

Figure 1. Working principle of the A-H PCR scheme. (A) Generation of single-stranded amplicons through 3′-specific extension. (B) Elimination of PD accumulation through the thermodynamically preferred single-stranded panhandle structure.

Ability of A-H PCR to Produce ss-Amplicons. We first verified the ability of the A-H PCR to produce ss-amplicons using singleplex PCR. A sequence of 192 base pairs (bp) encompassing rs2252992 was amplified using HANDS, asymmetric PCR, and A-H PCR (Table S1). Agarose gel analysis showed that HANDS produced a single band of ds-amplicons at approximately 230 bp, whereas asymmetric PCR and A-H PCR produced two bands: one at approximately 230 bp (upper band) and the other at approximately 180 bp (lower band) (Figure 2A). Sanger sequencing revealed that the former could be sequenced using both the forward and reverse primers, whereas the latter could be sequenced using only the forward primer. Therefore, we concluded that the upper band represents ds-amplicons, whereas the lower band represents ss-amplicons (Figure 2B).

To verify the existence of ss-amplicons in the A-H PCR, a stem-shared molecular beacon oriented in the same direction as the forward primer was added to the above reactions. Real-time PCR detection showed that the cycle threshold (Ct) values were in the order of HANDS < asymmetric PCR < A-H PCR (Figure 2C, left), and the melting peak heights were in the order of HANDS < A-H PCR < asymmetric PCR (Figure 2C, right). These results revealed that symmetric HANDS showed higher amplification efficiency than A-H PCR and asymmetric PCR, as indicated by the smaller Ct required to

https://doi.org/10.1021/acs.analchem.4c01322
Anal. Chem. 2024, 96, 9200−9208

Tecan Ex. 2142, Page 3 of 9
QIAGEN Sciences, LLC v. Tecan Genomics - IPR2025-00028

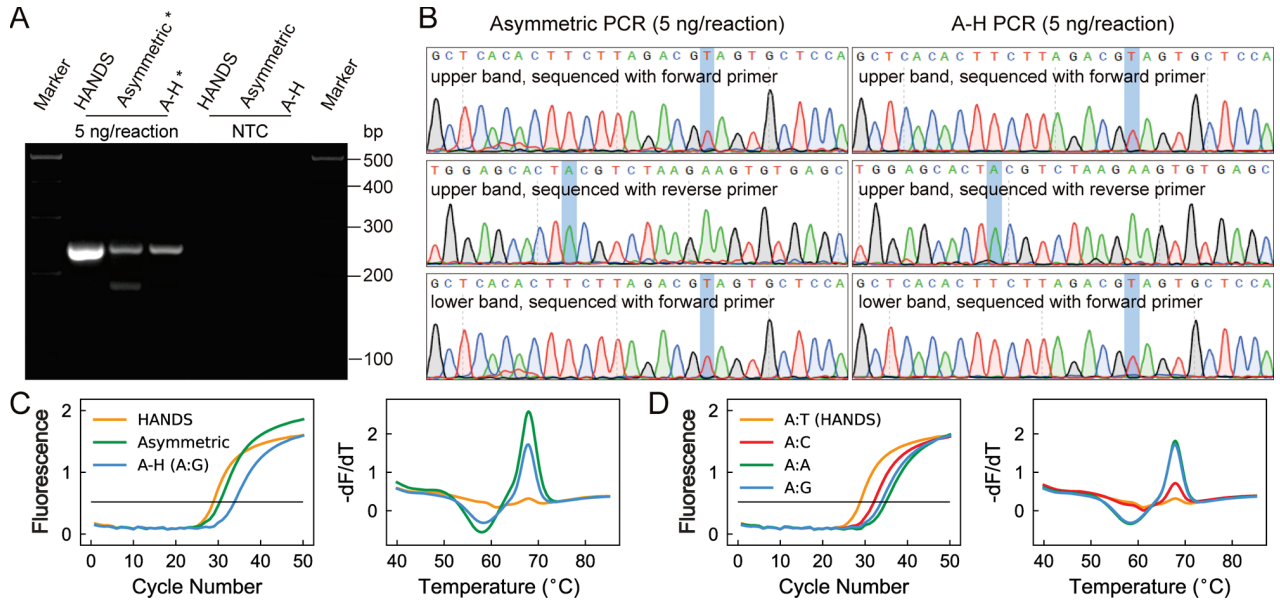

Figure 2. Comparison of HANDS, asymmetric PCR, and A-H PCR in the production of ss-amplicons. (A) PCR product analysis using 4% agarose gel electrophoresis. The products of the reactions labeled with "*" were further sequenced. (B) Sanger sequencing results of two bands produced by asymmetric PCR and A-H PCR. The displayed sequences represent the probe-binding region, and the shadowed nucleotides indicate SNPs. (C) Amplification curves (left) and melting curves (right) generated by the three different PCRs. The Ct values of HANDS, asymmetric PCR, and A-H PCR were 28.83, 30.35, and 33.86, respectively. (D) Amplification curves (left) and melting curves (right) generated by changing the 3′-end nucleotide of the tail carried by the forward primer. The Ct values of the A:T match, A:C, A:A, and A:G mismatches were 28.83, 32.09, 34.90, and 33.86, respectively.

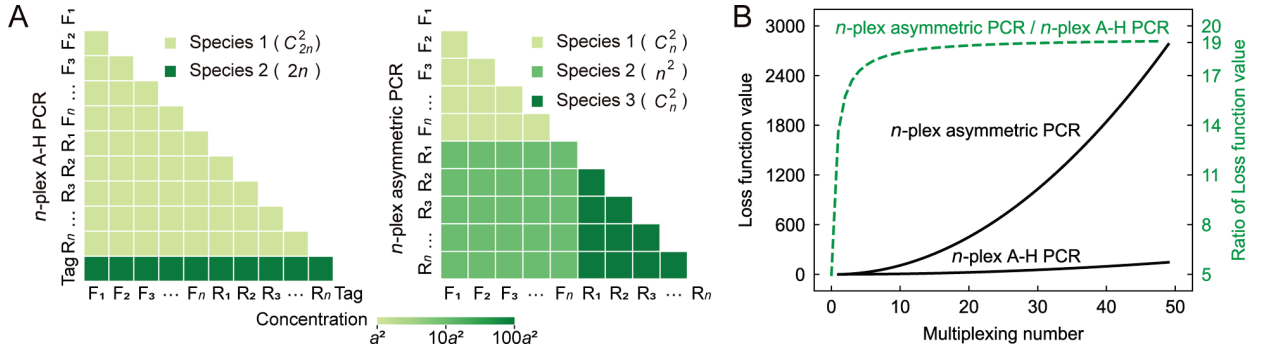

Figure 3. Analysis of PD interactions. (A) Species and concentration of PDs for *n*-plex A-H PCR and *n*-plex asymmetric PCR according to primer concentrations. For an *n*-plex A-H PCR, the concentration of the Tag primer is 100 times to that of the tailed primers. For an *n*-plex asymmetric PCR, the concentration of reverse primers is 10 times to that of forward primers. The PD number for each species is listed near the corresponding species. The concentration of PD for two primers is represented by the color of the heatmap. F: forward primer, R: reverse primer, and *a*: the concentration of tailed primer of A-H PCR or that of forward primer of asymmetric PCR. (B) Relationship between loss function value and multiplexing number for *n*-plex A-H PCR and *n*-plex asymmetric PCR.

produce a positive signal. Conversely, A-H PCR and asymmetric PCR produced more ss-amplicons than symmetric HANDS, as revealed by the higher melting peaks produced from the hybridization of ss-amplicons and molecular beacons.

We then investigated the influence of the mismatch type on the production of ss-amplicons in A-H PCR. Three A-H PCRs with different mismatched base pairs (A:C, A:A, and A:G) were compared with the HANDS (Table S2). Real-time PCR detection showed that the Ct values were in the order of A:T (HANDS) < A:C < A:G ≈ A:A (Figure 2D, left), and the melting peak heights were in the order of A:T < A:C < A:G ≈ A:A (Figure 2D, right). These results showed that a larger Ct and higher melting peak indicated more ss-amplicons in the A-H PCR. We attributed this difference to asymmetric amplification driven by the Tag primer, given that these PCRs used identical concentrations of tailed primers and had equivalent symmetric amplification. To test this hypothesis, we recovered the ds-amplicons from the four PCRs and, after calibrating to an equal concentration (1×10^4 copies/μL), subjected them to a second 56-cycle PCR using the Tag primer alone in the presence of SYTO 9 (Text S1). The Ct values obtained were in the order A:T < A:C < A:A ≈ A:G (Figure S1). This order reflects the diminishing ability of the Tag primer to extend along the one-nucleotide mismatched strands. As the A:C mismatch gave a Ct value much closer to that of the A:T match, it functioned more like a matched base pair that favored exponential amplification and generated more ds-amplicons. In comparison, A:A and A:G mismatches were more resistant to the one-nucleotide mismatched extension, thus favoring linear amplification and generating more ss-

https://doi.org/10.1021/acs.analchem.4c01322
Anal. Chem. 2024, 96, 9200−9208

Tecan Ex. 2142, Page 4 of 9
QIAGEN Sciences, LLC v. Tecan Genomics - IPR2025-00028

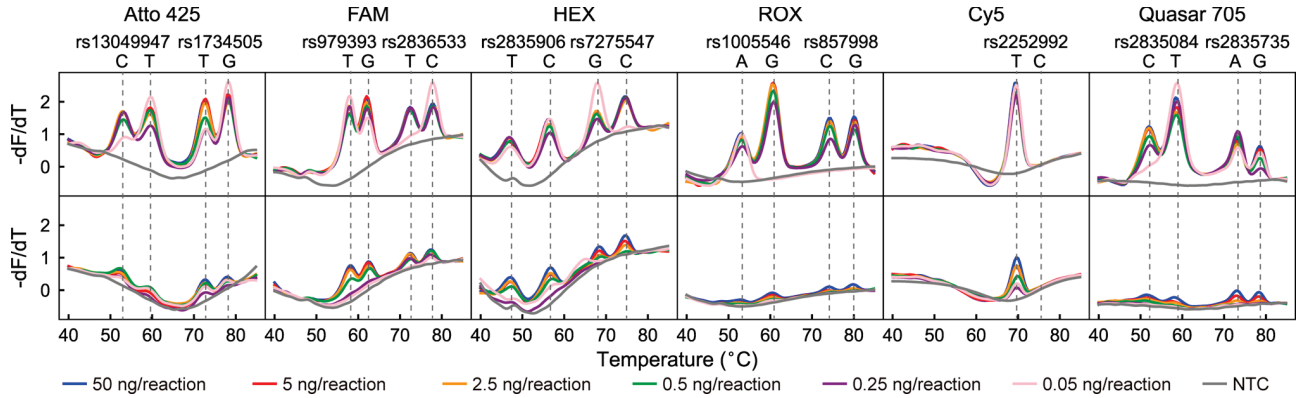

Figure 4. Melting curves of 11-plex A-H PCR (upper panel) and 11-plex asymmetric PCR (lower panel) using different amounts of gDNA.

amplicons. Consequently, these results revealed that A:A and A:G mismatches are more destabilizing than A:C mismatches and are more effective in producing ss-amplicons in A-H PCR.

Reduced PD Formation in A-H PCR. In a multiplex PCR, there are three major factors that determine the severity of PD formation, including the number of primer−primer interactions (i.e., PDs), primer concentrations, and primer sequences. An n-plex A-H PCR contains $2n$ tailed primers of low concentration (a) and one Tag primer of high concentration (b). Thus, the PDs have two dominant species: species 1 is formed between tailed primers and has a number of C_{2n}^2; species 2 is formed between tailed primers and the Tag primer and has a number of $2n$ (Figure 3A, left). In comparison, an n-plex asymmetric PCR contains n limiting primers (forward primers) of low concentration (a) and n excess primers (reverse primers) of high concentration (c). Thus, the PDs have three dominant species: species 1 is formed between limiting primers and has a number of C_n^2; species 2 is formed between limiting primers and excess primers and has a number of n^2; and species 3 is formed between excess primers and has a number of C_n^2 (Figure 3A, right).

According to Xie et al.,[18] the predicted formation of PDs for two primers can be defined as the Badness value derived from their sequences. By summing the product of concentration and Badness value of each PD, the Loss function value, which is proposed to approximate the severity of PD formation for a multiplex PCR, could be obtained for the n-plex A-H PCR and n-plex asymmetric PCR, respectively, as follows:

$$\text{Loss function value}_{n-\text{plex A-H PCR}} = C_{2n}^2 \times a^2 \times \text{Badness1} + 2n \times ab \times \text{Badness2} \quad (1)$$

where Badness 1 and 2 are the average Badness value of species 1 and 2 of A-H PCR, respectively. Badness 3 is the average Badness value of the three species of asymmetric PCR.

$$\text{Loss function value}_{n-\text{plex asymmetric PCR}} = (C_n^2 \times a^2 + n^2 \times ac + C_n^2 \times c^2) \times \text{Badness3} \quad (2)$$

To further compare the severity of PD formation, the loss function values for n-plex A-H PCR and n-plex asymmetric PCR were calculated for the different multiplexing numbers (n) by referring to the average parameters (i.e., primer concentrations and sequences) of the 11-plex A-H PCR and the 11-plex asymmetric PCR in this study (Table S4). For the n-plex A-H PCR, a = 0.04 μM, b = 0.2n μM, Badness 1 = 13.17, and Badness 2 = 1.14. For the n-plex asymmetric PCR, a = 0.04 μM, c = 0.4 μM, and Badness 3 = 12.16. By plotting the Loss function value against n, we could infer that the Loss function value of n-plex asymmetric PCR increases at a much higher amplitude than that of n-plex A-H PCR as n increases. The ratio reached a plateau of approximately 19 when n > 10 (Figure 3B). Consequently, A-H PCR showed approximately 19-fold lower PD formation than asymmetric PCR in >10-plex amplification.

Enhanced Analytical Sensitivity of A-H PCR. A reduction in PD formation should lead to enhanced detection sensitivity of multiplex PCR. We verified this hypothesis by designing an 11-plex A-H PCR combined with multicolor melting curve analysis (MMCA)[3] for genotyping 11 SNPs located in the down syndrome critical region (DSCR) on chromosome 21. For better resolution, the T_m differences (ΔT_m) between adjacent melting peaks in each channel were set at >4.5 °C. For comparison, an 11-plex asymmetric PCR was designed using identical specific primers and probes but by removing the Tag primer and all tail sequences in the primers (Table S4). According to the primer sequences and concentrations used in the reactions, the loss function values of 11-plex A-H PCR and 11-plex asymmetric PCR were calculated as 16.64 and 356.64, respectively. Overall, 11-plex A-H PCR resulted in 21.43 (356.64/16.64)-fold lower PD formation than 11-plex asymmetric PCR. We then examined whether reduced PD formation could lead to increased analytical sensitivity. For this purpose, we prepared a series of template solutions containing human gDNA at concentrations of 0.01, 0.05, 0.1, 0.5, 1.0, and 10 ng/μL and detected each with four replicates in both multiplex reactions. The 11-plex A-H PCR displayed much higher and more balanced melting peaks than those of 11-plex asymmetric PCR when identical template amounts were used (Figure 4). Moreover, the former could repeatedly gain the genotypes of 11 SNPs with template amounts as low as 0.25 ng/reaction, whereas the latter could only achieve this for template amounts of at least 5.0 ng/reaction (Figure S2B). In other words, 11-plex A-H PCR was 20-fold more sensitive than 11-plex asymmetric PCR. In parallel, the amplification curves of 11-plex A-H PCR gave a higher fluorescence amplitude and were more converged at the end of the PCR than their counterparts (Figure S2A,C), indicating that more specific amplicons were generated when amplification was complete.

We further verified whether the increased analytical sensitivity in A-H PCR could also be extended to higher

https://doi.org/10.1021/acs.analchem.4c01322
Anal. Chem. 2024, 96, 9200−9208

Tecan Ex. 2142, Page 5 of 9
QIAGEN Sciences, LLC v. Tecan Genomics - IPR2025-00028

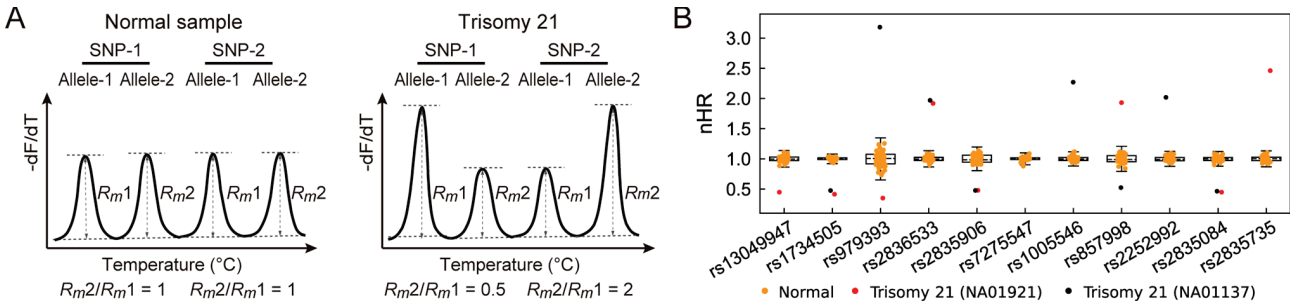

Figure 5. Allele quantification of multiple SNPs using 11-plex A-H PCR. (A) Theoretical melting curve of two heterozygous SNPs in normal and trisomy 21 gDNA samples. The overrepresented alleles in trisomy 21 are indicated by increased melting peak heights. (B) Normalized height ratio (nHR) values of heterozygous SNPs obtained from 87 normal gDNA samples and two trisomy 21 gDNA samples. The line within the box represents the median, and the horizontal borders of each box represent the interval between the 25th and 75th percentiles. Whiskers represent 3 standard deviations (3 SDs). Dots indicate all individual data points.

orders of multiplex reaction. For this purpose, we first prepared a 12-plex A-H PCR to detect 12 forensic SNPs, and then by gradually adding tailed-specific primers designed for other forensic SNPs to the 12-plex A-H PCR, we generated 36-plex, 60-plex, 84-plex, and 108-plex A-H PCRs (Table S5), respectively. Considering the limited number of melting peaks detectable in one reaction, we only observed amplification curves and melting curves using the corresponding probes of the initial 12 SNPs regardless of the multiplex orders. With the increase of multiplexing numbers, both the amplification curves and the melting curves of 12 SNPs could be repeatedly obtained despite a slight and sequential decrease in their signal amplitudes (Figure S3A). We then determined the lowest detectable gDNA required for the 108-plex A-H PCR. By detecting a series of template solutions containing human gDNA of 0.01, 0.05, 0.1, 0.5, 1.0, and 10 ng/μL each in four replicates, the 108-plex A-H PCR could repeatedly generate the genotypes of 12 loci when input gDNA amounts were 0.5 ng/reaction and above (Figure S3B). This lowest detectable concentration was very close to that (0.25 ng/reaction) of the 11-plex A-H PCR.

Balanced Amplification of A-H PCR. Unbiased amplification is a prerequisite for target quantification in a multiplex amplification system, which can be examined by allele quantification in the case of SNPs detection. Accordingly, we prepared a series of mixtures containing varied allele ratios of SNPs and tested whether they could be maintained after A-H PCR. Considering that a heterozygous biallelic SNP in normal gDNA has an allele ratio of 1.0 and a heterozygous biallelic SNP in trisomy 21 gDNA has an allele ratio of 0.5 (SNP-1 type) or 2 (SNP-2 type) (Figure 5A), we detected 87 normal gDNA samples and 2 trisomy 21 gDNA reference samples using 11-plex A-H PCR. In line with theoretical expectations, the nHR values of the two melting peaks obtained from each heterozygous SNP were close to 1.0 (standard deviation [SD] = 0.02−0.12) for the normal gDNA samples and 0.5 or 2.0 for the 2 trisomy 21 gDNA samples, respectively (Figure 5B and Table S7). These results were independent of sample sources and extraction methods (Figure S4 and Table S8). To further explore the resolution of A-H PCR for quantification of allele ratios, we prepared a series of normal gDNA samples containing different percentages of the trisomy 21 gDNA. The results showed that for all seven heterozygous SNPs found in the gDNA samples, the nHR values either decreased (SNP-1 type) or increased (SNP-2 type) as the percentages of trisomy 21 increased (Figure S5). The sample containing 20% trisomy 21 gDNA was clearly distinct from the normal sample. Next, we investigated whether the allele ratio was stable with different amounts of DNA template. We detected four normal gDNA and two trisomy 21 gDNA reference samples in different amounts: 250, 125, 50, and 25 ng/reaction. The nHR of normal and trisomy 21 gDNA showed an unequivocal distinction across all concentrations (Figure S6). The above results confirmed that A-H PCR could stably amplify all the targets and maintain the allele ratios regardless of the sample sources, DNA extraction methods, and DNA input concentrations. Finally, a 5-plex A-H PCR was established and coupled with the 11-plex A-H PCR. This assay targeted a total of 16 SNPs in DSCR and was used to identify trisomy 21 samples in 234 amniotic fluid and 108 chorionic villus samples in a blind manner. The results showed that all 31 trisomy 21 samples were correctly picked up by comparing with their medical records (Text S2).

DISCUSSION

In the present study, a generic multiplex asymmetric PCR approach, A-H PCR, was developed by coupling ARMS with HANDS in a single reaction. This was achieved by introducing an oligonucleotide sequence, which was present as both a Tag primer and a tail at the 5′-end of all the target-specific primers, with the exception of a one-nucleotide difference at the 3′-end of the tail for each primer pair. Since equal amounts of forward and reverse primers were used, extensive optimization involved in conventional asymmetric PCR was largely avoided. By taking advantage of the alleviation of PD accumulation, efficient target amplification is ensured, sensitive detection, and stable allele amplification are achieved.

The A-H PCR is an asymmetric PCR scheme that utilizes equimolar amounts of forward and reverse primers throughout the reaction. These primers can generate ds-amplicons in the initial cycles, similar to conventional asymmetric PCR. Accordingly, many experimental optimizations, such as primer ratio or T_m adjustment of the limiting primers, commonly involved in traditional asymmetric PCRs, are largely avoided. A-H PCR achieves asymmetric amplification by selective extension of the Tag primer along the matched strands, and thus relies on its 3′-end specificity as ARMS. The A:G and A:A mismatches displayed higher melting peaks than the A:C mismatch, suggesting that these purine:purine mismatches generated more ss-amplicons than the purine:pyrimidine mismatches (Figure 2D). Moreover, this phenomenon was observed in ARMS, in which purine:purine or pyrimidine:pyr-

https://doi.org/10.1021/acs.analchem.4c01322
Anal. Chem. 2024, 96, 9200−9208

Tecan Ex. 2142, Page 6 of 9
QIAGEN Sciences, LLC v. Tecan Genomics - IPR2025-00028

imidine mismatches were considerably more refractory to extension than purine:pyrimidine mismatches, leading to more discriminative detection.[19] According to thermodynamics, pyrimidine:pyrimidine mismatches are more destabilizing in all sequence contexts[20,21] and may be better used for A-H PCR. ARMS commonly introduces an additional mismatch near the 3′-end of the primer to increase specificity, and we speculated that an additional mismatch at the 3′-end of the tail might further facilitate the production of ss-amplicons in A-H PCR. Future studies are needed to test these hypotheses, although a single purine:purine mismatch was sufficient to successfully perform A-H PCR in our study.

PDs in multiplex PCR significantly influence the specific amplification, leading to a substantial loss in analytical sensitivity. HANDS inhibits PD accumulation by adding a homo-oligonucleotide to all primers to generate the panhandle structure.[15] In comparison, A-H PCR has a pair of mismatches at the 3′-end of the tail, and this modification does not affect panhandle structure formation, considering that the tail length can be arbitrarily adjusted. Similar to the HANDS, A-H PCR has two mechanisms for reducing PD formation. One is the panhandle structure of PDs, which can inhibit PD accumulation by preventing access of the Tag primer for exponential amplification. The other is the combined use of low concentrations of tailed-specific primers and a high concentration of the Tag primer, which minimizes the interactions between primers, substantially reducing the Loss function value of the multiplex PCR. Consequently, sensitive detection was achieved in the entire range of multiplex order from 11-plex to 108-plex. To the best of our knowledge, only one study has reported a 10-plex asymmetric PCR-based microarray assay with a detection limit of approximately 6.60 ng per reaction.[17] The detection limit was more than 10-fold higher than that of A-H PCR, regardless of its multiplexing order.

Furthermore, the reduction of PD helped protect ss-amplicon generation from the effects of nonspecific amplification, rendering stable and accurate allele amplification of the original template. This was demonstrated through the genotyping of 11 biallelic SNPs using MMCA, where a sample containing 20% trisomy 21 could be discriminated from a normal sample. Such distinct allele quantification was reproducible when tested with gDNA from different sources and extraction methods, factors that might otherwise affect the reproducibility of other quantitative approaches for copy number detection.[22] The quantitative feature of A-H PCR was successfully used to design a trisomy 21 assay, with the correct identification of 31 trisomy 21 cases in 342 clinical samples, A-H PCR improved the number of quantitative SNP loci in a single reaction from two[19] to 11 in our study. Regarding the maintained analytical sensitivity in even higher order of multiplex, A-H PCR could accommodate much more SNPs loci for quantification in one reaction. Also, balanced allele amplification would be beneficial for detecting mutation abundance.[23−25]

Although we have demonstrated the advantages mentioned above, the use of A-H PCR warrants further investigation. First, due to the limited number of melting peaks detectable in a single detection channel and the confined fluorescence channels on a real-time PCR thermocycler, our study only detected a small number of SNPs in one reaction using A-H PCR. For instance, in a high-order multiplex A-H PCR, e.g., 108 A-H PCR, we only detected 12 SNPs, leaving the detectability of other SNPs unconfirmed. Nevertheless, the balanced amplification observed in A-H PCR lead us to believe that the detection of all SNPs could be feasible if their respective probes were included in the reaction. This hypothesis is further supported by the nearly consistent detection sensitivity observed across the entire range of multiplexing (from 11- to 108-plex) in our study. Second, A-H PCR has not been evaluated with alternative detection schemes, such as liquid chip,[26] microarray,[27] or digital melting PCR,[4] which all require ss-amplicons for probe hybridization. It is conceivable that these detection schemes could also benefit from enhanced sensitivity and quantitative capability considering the increased and balanced ss-amplicons provided by A-H PCR. Of note, among these platforms, only melting curve analysis allows for closed-tube detection with a short turnaround time, ease of use, and no risk of carryover contamination, and all of these features are favorable in clinical and research settings. Despite its current limitations, with the advent of a multicolor real-time thermocycler (e.g., 10-color),[28] more targets could be expectedly detected through melting curve analysis in the future.

CONCLUSIONS

PD formation and unequal amplification rates present significant obstacles in multiplex asymmetric PCR. Our study demonstrates that by integrating two classical PCR schemes, ARMS and HANDS, we can asymmetrically amplify multiple targets while eliminating PD accumulation. This innovative approach enables multiplex asymmetric PCR to achieve sensitive and quantitative detection by avoiding nonspecific amplification and ensuring balanced amplification. A-H PCR proves particularly beneficial in scenarios where template material is scarce, a common issue in both clinical and research environments. The balanced amplification provided by A-H PCR preserves the allele composition of the input DNA, offering a quantitative advantage for various scenarios. Consequently, we foresee that A-H PCR will not only improve current asymmetric amplification techniques but also advance multiplex detection in a variety of untapped applications.

ASSOCIATED CONTENT

Supporting Information

The Supporting Information is available free of charge at https://pubs.acs.org/doi/10.1021/acs.analchem.4c01322.

Supplementary Text S1−S2, Tables S1−S11, Figures S1−S7: experimental details; trisomy 21 identification; the sequence of synthetic primers and probes (PDF)

AUTHOR INFORMATION

Corresponding Authors

Qiuying Huang − *Engineering Research Centre of Molecular Diagnostics of the Ministry of Education, State Key Laboratory of Cellular Stress Biology, State Key Laboratory of Molecular Vaccinology and Molecular Diagnostics, School of Life Sciences, Xiamen University, Xiamen 361102, China*; Email: hqying@xmu.edu.cn

Qingge Li − *Engineering Research Centre of Molecular Diagnostics of the Ministry of Education, State Key Laboratory of Cellular Stress Biology, State Key Laboratory of Molecular Vaccinology and Molecular Diagnostics, School of Life Sciences, Xiamen University, Xiamen 361102, China*; Email: qgli@xmu.edu.cn

Tecan Ex. 2142, Page 7 of 9
QIAGEN Sciences, LLC v. Tecan Genomics - IPR2025-00028

Authors

Ying Liu − *Engineering Research Centre of Molecular Diagnostics of the Ministry of Education, State Key Laboratory of Cellular Stress Biology, State Key Laboratory of Molecular Vaccinology and Molecular Diagnostics, School of Life Sciences, Xiamen University, Xiamen 361102, China;* orcid.org/0009-0008-8265-7204

Yinghua Liu − *Centre for Reproduction and Genetics, Suzhou Municipal Hospital, The Affiliated Suzhou Hospital of Nanjing Medical University, Suzhou 215002, China*

Liu Guo − *Engineering Research Centre of Molecular Diagnostics of the Ministry of Education, State Key Laboratory of Cellular Stress Biology, State Key Laboratory of Molecular Vaccinology and Molecular Diagnostics, School of Life Sciences, Xiamen University, Xiamen 361102, China*

Yazhe Wu − *Engineering Research Centre of Molecular Diagnostics of the Ministry of Education, State Key Laboratory of Cellular Stress Biology, State Key Laboratory of Molecular Vaccinology and Molecular Diagnostics, School of Life Sciences, Xiamen University, Xiamen 361102, China*

Yafang Wang − *Engineering Research Centre of Molecular Diagnostics of the Ministry of Education, State Key Laboratory of Cellular Stress Biology, State Key Laboratory of Molecular Vaccinology and Molecular Diagnostics, School of Life Sciences, Xiamen University, Xiamen 361102, China*

Lingzhen Xu − *Engineering Research Centre of Molecular Diagnostics of the Ministry of Education, State Key Laboratory of Cellular Stress Biology, State Key Laboratory of Molecular Vaccinology and Molecular Diagnostics, School of Life Sciences, Xiamen University, Xiamen 361102, China*

Mingzhu Xu − *Engineering Research Centre of Molecular Diagnostics of the Ministry of Education, State Key Laboratory of Cellular Stress Biology, State Key Laboratory of Molecular Vaccinology and Molecular Diagnostics, School of Life Sciences, Xiamen University, Xiamen 361102, China*

Siyu Huang − *Engineering Research Centre of Molecular Diagnostics of the Ministry of Education, State Key Laboratory of Cellular Stress Biology, State Key Laboratory of Molecular Vaccinology and Molecular Diagnostics, School of Life Sciences, Xiamen University, Xiamen 361102, China*

Ping Chen − *NHC Key Laboratory of Thalassemia Medicine, Key Laboratory of Thalassemia Medicine, Chinese Academy of Medical Sciences, Guangxi Key Laboratory of Thalassemia Research, The First Affiliated Hospital of Guangxi Medical University, Nanning 530021, China*

Ting Wang − *Centre for Reproduction and Genetics, Suzhou Municipal Hospital, The Affiliated Suzhou Hospital of Nanjing Medical University, Suzhou 215002, China*

Complete contact information is available at: https://pubs.acs.org/10.1021/acs.analchem.4c01322

Author Contributions

#Y.L. and Y.H.L. contributed equally to this work.

Notes

The authors declare no competing financial interest.

■ ACKNOWLEDGMENTS

This work was supported by the National Natural Science Foundation of China [82271729]; Key Biosafety Research and Development Technology Project [2021YFC1200200]; the Scientific and Technological Assistance Projects to Developing Countries [KY202002008]; the Science and Technology Planning Projects of Guangxi Province-Specific Research Project of Guangxi for Research Bases and Talents [AD23026025]; the Science and Technology Planning Projects of Liuzhou City [2023YRZ0103]; Natural Science Foundation of Xiamen Municipality [3502Z20227172]; the Guangxi Key Laboratory Thalassemia Research Project [22-035-24]; and the Innovation Laboratory Project of Xiangan, Xiamen [2023XAKJ0103068].

■ REFERENCES

(1) Gyllensten, U. B.; Erlich, H. A. *Proc. Natl. Acad. Sci. U. S. A.* **1988**, *85*, 7652−7656.
(2) Lay, M. J.; Wittwer, C. T. *Clin. Chem.* **1997**, *43*, 2262−2267.
(3) Huang, Q.; Liu, Z.; Liao, Y.; Chen, X.; Zhang, Y.; Li, Q. *PLoS One* **2011**, *6*, No. e19206.
(4) Luo, Y.; Cui, X.; Cheruba, E.; Chua, Y. K.; Ng, C.; Tan, R. Z.; Tan, K. K.; Cheow, L. F. *Small Methods* **2022**, *6*, No. e2200185.
(5) Liu, F.; Liu, H.; Liao, Y.; Wei, J.; Zhou, X.; Xing, D. *Biosens. Bioelectron.* **2015**, *74*, 778−785.
(6) Sonkar, S. C.; Sachdev, D.; Mishra, P. K.; Kumar, A.; Mittal, P.; Saluja, D. *Biosens. Bioelectron.* **2016**, *86*, 41−47.
(7) Wang, D.; Gao, H.; Zhang, R.; Ma, X.; Zhou, Y.; Cheng, J. *Biotechniques* **2003**, *35*, 300−308.
(8) Poddar, S. K. *Mol. Cell Probes* **2000**, *14*, 25−32.
(9) Sanchez, J. A.; Pierce, K. E.; Rice, J. E.; Wangh, L. J. *Proc. Natl. Acad. Sci. U. S. A.* **2004**, *101*, 1933−1938.
(10) Jia, H.; Chen, Z.; Wu, H.; Ye, H.; Yan, Z.; Zhou, G. *Analyst* **2011**, *136*, 5229−5233.
(11) Reddy Banda, S.; Klapproth, H.; Smit, N.; Bednar, S.; Brandstetter, T.; Rühe, J. *Front. Bioeng. Biotechnol.* **2022**, *10*, No. 1045154.
(12) Tolnai, Z.; Harkai, Á; Szeitner, Z.; Scholz, É. N.; Percze, K.; Gyurkovics, A.; Mészáros, T. *Anal. Chim. Acta* **2019**, *1047*, 225−230.
(13) Fan, J. B.; Chee, M. S.; Gunderson, K. L. *Nat. Rev. Genet.* **2006**, *7*, 632−644.
(14) Lin, Z.; Cui, X.; Li, H. *Proc. Natl. Acad. Sci. U. S. A.* **1996**, *93*, 2582−2587.
(15) Brownie, J.; Shawcross, S.; Theaker, J.; Whitcombe, D.; Ferrie, R.; Newton, C.; Little, S. *Nucleic Acids Res.* **1997**, *25*, 3235−3241.
(16) Shapero, M. H.; Zhang, J.; Loraine, A.; Liu, W.; Di, X.; Liu, G.; Jones, K. W. *Nucleic Acids Res.* **2004**, *32*, No. e181.
(17) Zhu, L. X.; Zhang, Z. W.; Liang, D.; Jiang, D.; Wang, C.; Du, N.; Zhang, Q.; Mitchelson, K.; Cheng, J. *Antimicrob. Agents Chemother.* **2007**, *51*, 3707−3713.
(18) Xie, N. G.; Wang, M. X.; Song, P.; Mao, S.; Wang, Y.; Yang, Y.; Luo, J.; Ren, S.; Zhang, D. Y. *Nat. Commun.* **2022**, *13*, 1881.
(19) Pont-kingdon, G.; Lyon, E. *Clin. Chem.* **2003**, *49*, 1087−1094.
(20) Newton, C. R.; Graham, A.; Heptinstall, L. E.; Powell, S. J.; Summers, C.; Kalsheker, N.; Smith, J. C.; Markham, A. F. *Nucleic Acids Res.* **1989**, *17*, 2503−2516.
(21) Peyret, N.; Seneviratne, P. A.; Allawi, H. T.; Santalucia, J. *Biochemistry* **1999**, *38*, 3468−3477.
(22) Chen, X. W.; Li, Y. F.; Huang, Q. Y.; Lin, X. M.; Wang, X. D.; Wang, Y. F.; Liu, Y.; He, Q. S.; Liu, Y. H.; Wang, T.; Ji, Z. L.; Li, Q. G. *eBioMedicine* **2021**, *70*, No. 103535.
(23) Botezatu, I. V.; Nechaeva, I. O.; Stroganova, A. M.; Senderovich, A. I.; Kondratova, V. N.; Shelepov, V. P.; Lichtenstein, A. V. *Data Brief.* **2015**, *5*, 913−917.
(24) Xu, Y.; Liang, B.; Du, C.; Tian, X.; Cai, X.; Hou, Y.; Li, H.; Zheng, R.; Li, J.; Liu, Y.; Wang, K.; Ammar Athar, M.; Tan, Y.; Li, Q. *J. Clin. Microbiol.* **2019**, *57*, No. e01096-18, DOI: 10.1128/JCM.01096-18.
(25) Magyar, I.; Colman, D.; Arnold, E.; Baumgartner, D.; Bottani, A.; Fokstuen, S.; Addor, M. C.; Berger, W.; Carrel, T.; Steinmann, B.; Mátyás, G. *Hum. Mutat.* **2009**, *30*, 1355−1364.
(26) Chen, X.; Zhang, D. S.; Wang, L.; Guo, Q.; Xu, H.; Lou, J.; Gu, H. *J. Biomed. Nanotechnol.* **2019**, *15*, 1578−1588.

Tecan Ex. 2142, Page 8 of 9
QIAGEN Sciences, LLC v. Tecan Genomics - IPR2025-00028

(27) Erdogan, F.; Kirchner, R.; Mann, W.; Ropers, H. H.; Nuber, U. A. *Nucleic Acids Res.* **2001**, *29*, E36.
(28) Chakravorty, S.; Roh, S. S.; Glass, J.; Smith, L. E.; Simmons, A. M.; Lund, K.; Lokhov, S.; Liu, X.; Xu, P.; Zhang, G.; Via, L. E.; Shen, Q.; Ruan, X.; Yuan, X.; Zhu, H. Z.; Viazovkina, E.; Shenai, S.; Rowneki, M.; Lee, J. S.; Barry, C. E., III; Gao, Q.; Persing, D.; Kwiatkawoski, R.; Jones, M.; Gall, A.; Alland, D. *J. Clin. Microbiol.* **2017**, *55*, 183−198.

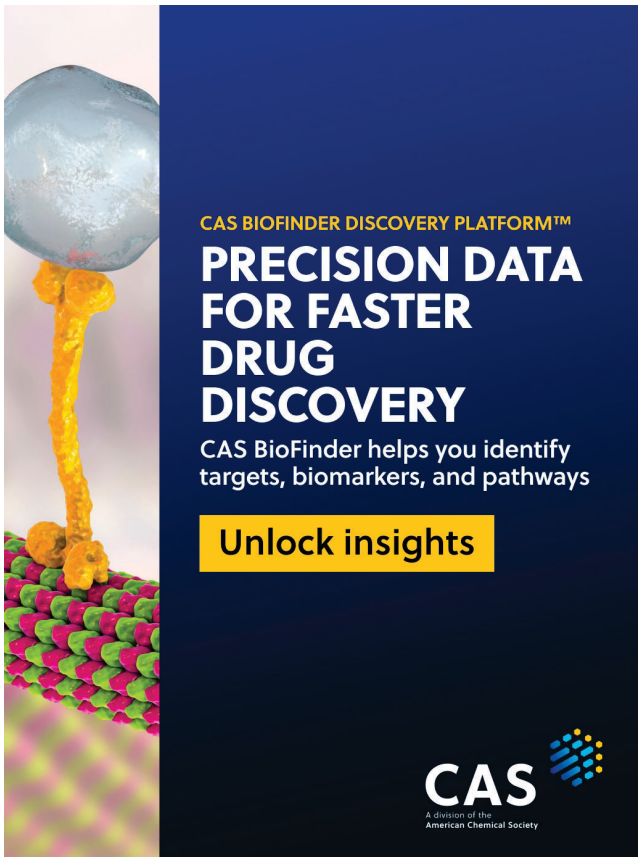

https://doi.org/10.1021/acs.analchem.4c01322
Anal. Chem. 2024, 96, 9200−9208